JOURNAL OF Applied Polymer SCIENCE

Solvent Inducing Aggregates of Perylene Tetracarboxylic Diimide in Polymer Backbone

Fan Kong,[1] Buwei Tang,[1] Xueqin Zhang,[1] Baoping Lin,[1] Teng Qiu[2]
[1]School of Chemistry and Chemical Engineering, Southeast University, Nanjing 211189, People's Republic of China
[2]Department of Physics, Southeast University, Nanjing 211189, People's Republic of China
Correspondence to: F. Kong (E-mail: kongfan@seu.edu.cn)

ABSTRACT: We have investigated the optical properties of a synthesized polymer containing perylene tetracarboxylic diimide (PDI) in different solvents. The structured absorption and photoluminescence (PL) spectra of the PDI in the polymer are sensitive to the solvents. The excited states with the PL peaks at 530 and 570 nm have the same PL excitation bands and life times, but the PL excitation band of the 625 nm excited states with long life time is different from the others. The PL bands with the peaks at 530 and 570 nm originate from the separated PDIs, whereas the 625 nm emission band is connected with the π–π stacked aggregates of the PDI in the polymer. The polymer chains become coiled to be favor of forming the π–π stacked aggregates of the PDI in weak polar solvent. The experimental results indicate that more π–π stacked aggregates are formed in tetrahydrofuran/ethanol blend solvents due to the collapsed polymer chains, but the PL intensity of the aggregates is precipitately decreased with the increase in the content of ethanol due to concentration quenching. © 2013 Wiley Periodicals, Inc. J. Appl. Polym. Sci. 000: 000–000, 2013

KEYWORDS: conducting polymers; optical properties; polyimides

accepted 23 June 2013; Published online
DOI: 10.1002/app.39687

INTRODUCTION

Perylene tetracarboxylic diimide derivatives (PDIs) have been extensively investigated due to their excellent optoelectronic properties, such as light fastness, intense photoluminescence (PL), and outstanding n-type semiconductivity.[1] These dyes and their assemblies have been applied in artificial light harvesting systems,[2,3] photoinduced electron transfer systems,[4,5] and organic electronic devices, such as organic light emitting diodes (OLEDs),[6,7] organic thin-film transistors (OTFT),[8] and solar cells.[9] Amount of the PDIs have been synthesized due to the facile chemical modification of the 1, 6, 7, 12 sites on perylene ring and imide groups.[10,11] The PDIs have been introduced into polymer chains to improve their optoelectronic properties, which have been applied in polymer solar cells and OTFTs.[12–14] Geng and coworkers have synthesized fluorene-thiophene oligomers with the PDI caps, which can form order nanostructures in several nanometers via self-assembly.[15] The donor-acceptor polymers or oligomers, such as oligo(*p*-phenylene vinylene)-PDI,[16,17] and polyfluorene-PDI copolymer,[18] have been synthesized and applied in organic solar cells with high performances.

The solubility of the polymer containing the PDIs is very important for its application in organic electronics. Incorporation of flexible segments into rigid PDI polymer backbones is an important way to improve the solubilities and PL properties of the polymers.[19–22] A mixture of perylene dianhydride (PDA) and 4,4′-(hexafluoroisopropylidene) diphthalic anhydride (6FDA) has been reacted with aromatic diamines to obtain the PDI polymer with good solubility and high photoconductivity.[23] Fluorene moiety introducing into the backbone of polyimide can effectively improve the thermal and electrical properties of the polymer, such as heat stability, high glass transition temperature, and low dielectric constant.[24,25]

The PDIs are favor of forming aggregates to affect their optical and electric properties due to strong π–π interaction. Usually, the PDI aggregates often reduce the electroluminescence efficiencies of organic light-emitting diodes and the power conversion efficiencies of organic solar cells. In the article, we have presented the formation of the PDI aggregates in the polymer induced by solvents. Normally, the polymer can be dissolved in the solvent as the interactions between the polymer chain segments and the solvent molecules are larger than those among the polymer chain segments. In the case, the polymer chains are separated and surrounded by the solvent molecules in the dilute solution. The large interaction between the polymer chain segments and the solvent molecules is in favor of forming the extended polymer chain conformation, and inversely, the coiled polymer chain conformation is formed. The polymer chain

Applied Polymer SCIENCE

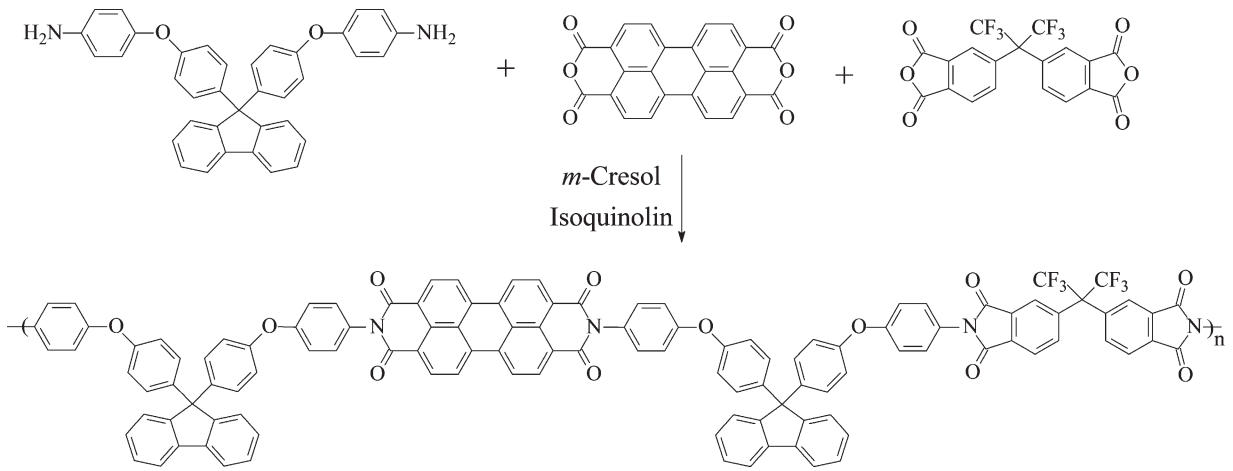

Figure 1. Synthetic route of the polymer.

conformation can be adjusted by adding nonsolvent into the polymer solution. As the nonsolvent is added, the extended polymer chain conformation becomes coiled, and then collapsed. Here, ethanol is used as the nonsolvent, which can be miscible with all portion of tetrahydrofuran (THF). Comparison with the chloroform solution, the aggregates of the PDI in the polymer are increased in the THF solution and result in an enhanced 625 nm emission band. Adding nonsolvent ethanol in the polymer solution can induce the formation of the PDI aggregates, but concentration quenching results in the decreased 625 nm emission band.

EXPERIMENTAL

Synthetic route of the polymer is shown in Figure 1. Perylene-3,4,9,10-tetracarboxylic acid dianhydride (PDA) and 4,4′-(hexafluoroisopropylidene) diphthalic anhydride (6FDA) were purchased from Aladdin Reagent Database. 9,9-bis[4-(4-amino-phenoxy)phenyl] fluorene (BAPF) was prepared from 9,9-bis(4-hydroxyphenyl)fluorene according to the literature.[26] BAPF (532.1 mg, 1 mmol), *m*-cresol (10 mL), and isoquinolin (0.2 mL) were added into a four-flask. After BAPF was dissolved, PDA (196 mg, 0.5 mmol) was added into the flask, and then, the reaction was performed under 180°C. After 8 h, the reaction system was cooled to room temperature. 6FDA (222 mg, 0.5 mmol) was added into the flask, and then reacted for 20 h under 180°C. The cooled reaction solution was slowly added into ethanol and the rough product was obtained by filtration. The product was purified by reprecipitating three times to obtain the red powder (0.788 g). Since, the 6FDA was introduced into the polymer chains with the same molar fraction of PDA, the synthesized polymer were well dissolved in many organic solvents, such as chloroform, *N*,*N*-dimethyl formamide, tetrahydrofuran (THF) and pyridine.

The number and mass average molecular weights of the polymer were measured to be 1.34×10^4 and 2.09×10^4 g/mol by gel permeation chromatography with reference of polystyrene. The polymer was dissolved in chloroform and THF to form the solutions with concentration of 2 mg/mL, respectively. The blend solvents were prepared from THF and ethanol. The contents of ethanol (v/v) in the blend solvents were 10, 20, 30, 40, and 50%, respectively. The polymer solutions were diluted in different solvents to form the solutions with the concentrations of 5×10^{-3} mg/mL for measuring ultraviolet-visible (UV–vis) absorption spectra and 5×10^{-4} mg/mL for measuring PL spectra. The PL spectra of the solutions were obtained by a FluoroLog-3 spectrophotometer (Horiba Jobin Yvon) with a Xe lamp. Time-resolved PL decay data were measured on the FluoroLog-3 spectrophotometer equipped with a time correlated single-photon counting (TCSPC) card. The UV–vis absorption spectra were acquired on a Shimadzu UV-3100 spectrophotometer. All the measurements were performed at room temperature.

RESULTS AND DISCUSSION

Figure 2 shows the UV–vis absorption spectra of the polymer in chloroform and THF. There are several structured absorption peaks in each absorption spectrum. The absorption band with a peak at 310 nm is connected with the electron transition in fluorene moieties, and its absorption intensities are similar in the chloroform and THF solutions. There are two characteristic

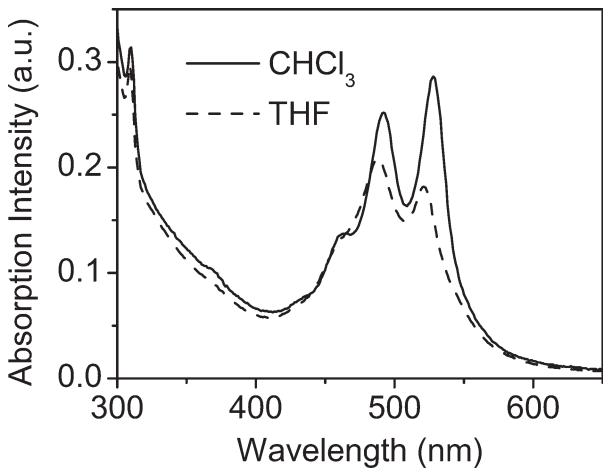

Figure 2. UV–vis absorption spectra of the polymer in chloroform and THF with the concentration of 5×10^{-3} mg/ml.

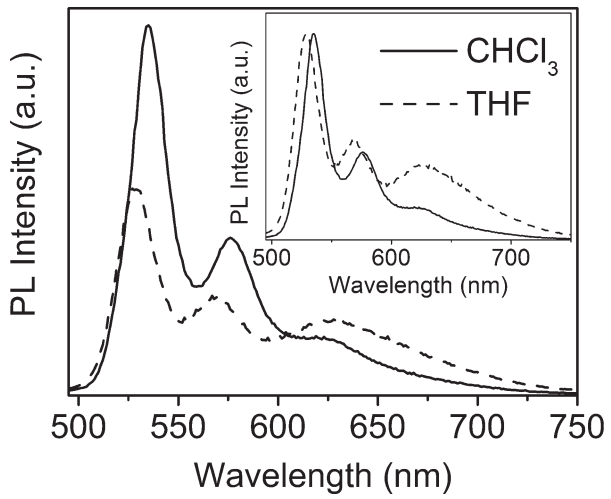

Figure 3. PL spectra of the PDI in the polymer chloroform and THF with the concentration of 5×10^{-4} mg/ml (excitation at 480 nm), the inset is the normalized PL spectra.

absorption bands with the peaks at 493 nm (0–1 transition) and 529 nm (0–0 transition) in the chloroform solution, which originate from π-electron transitions in the PDI. The absorption peaks of the PDI are blue shifted slightly in the THF solution. It can be seen that the absorption intensity of the PDI in the polymer in THF is lower than that in chloroform, especially for the 0–0 transition. According to Figure 2, the molar absorption coefficients (ε) of the PDI in the polymer in chloroform and THF are calculated to be 7.66×10^5 and 4.87×10^5 L/mol cm, respectively. The high molar absorption coefficients of the PDI in the polymer can efficiently absorb light, which is useful for its application in optoelectronics. Normally, the strong affinity between the imide group and chloroform facilitates the polymer to be dissolved. As a result, the polymer chains are extended in chloroform, corresponding to the strong optical absorption.

Figure 3 shows the PL spectra of the PDI in the polymer solutions. There are three well-structured peaks in each PL spectrum. Obviously, the emission intensity of the chloroform solution is higher than that of the THF solution, corresponding to larger molar absorption coefficient. It can be found that the main PL peak of the chloroform solution is red-shifted to 535 nm relative to the THF solution (529 nm) due to the effect of the solvent cage. Normally, the dipole moment of a fluorescent molecule is higher in the excited state than in the ground state due to intramolecular charge transfer. Therefore, following excitation, the solvent cage undergoes a relaxation, leading to a relaxed state of minimum free energy.[27] As a result, the red shifted emission from the PDI is observed in chloroform with a high polarity. As shown in Table I, the stokes shift of the PDI in the polymer is larger in THF than that in chloroform, which indicates that the solvation energy of the PDI in former is larger than that in later. The solvation energy is not only dependent on the dipole moment, polarizability, transition moment, and hydrogen bonding capability of the PDI, but also the dielectric constant, refractive index, and hydrogen bonding capability of the solvent molecule. It can be seen from the normalized PL spectra in the inset of Figure 3 that the relative intensity of the

Table I. Optical Parameters of the PDI in the Polymer in Chloroform and THF

	Abs (eV)	PL (eV)	Stokes shift (eV)	ε[a] (L/mol cm)
$CHCl_3$	2.344	2.318	0.026	7.66×10^5
THF	2.375	2.344	0.031	4.87×10^5

[a] The values are calculated from the absorption and PL at the 0-0 transition.

shoulder PL peak at 625 nm of the THF solution is much higher than that of the chloroform solution. The wide emission band with the peak at 625 nm is usually considered to be connected with the π–π stacked aggregates.[28] The enhanced 625 nm emission indicates that there are more π–π stacked aggregates of the PDIs formed in THF than in chloroform. In the dilute solution, the polymer chains are separated by the solvent molecules. The π–π stacked aggregates of the PDIs must be formed in a single polymer chains. In the case, the coiled polymer chains are in favor of forming the π–π stacked aggregates. The enhanced emission from the π–π stacked aggregates implies that there is the coiled polymer chain conformation in THF. Since, the two PDIs form the π–π stacked aggregates with strong interaction, the dipole moment of the PDI aggregate is changed a little bit in the excited state relative to that in the ground state. The effect of the solvent cage on the excited states in the aggregates becomes very little, and then, the emission peak of the π–π stacked aggregates is not obvious shift in different solvents.

For analyzing the origins of the excited states of the PDI in the polymer, the PL excitation (PLE) spectra are measured at the monitoring emission wavelengths of 530, 570, and 625 nm, respectively. As shown in Figure 4, the shapes of the PLE spectra measured at the monitoring emission wavelengths of 530 and 570 nm are both similar to the absorption of the separated PDIs,[29] indicating that the two excited states originate from the same π-electron transition absorption in the separated PDIs.

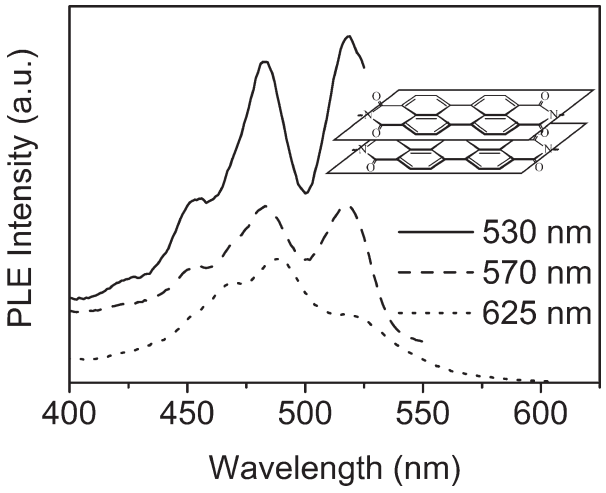

Figure 4. PLE spectra of the PDI in the polymer in THF measured at the monitoring emission wavelengths of 530, 570, and 625 nm, respectively. The inset is the schematic structure of the PDI π–π stacked aggregate.

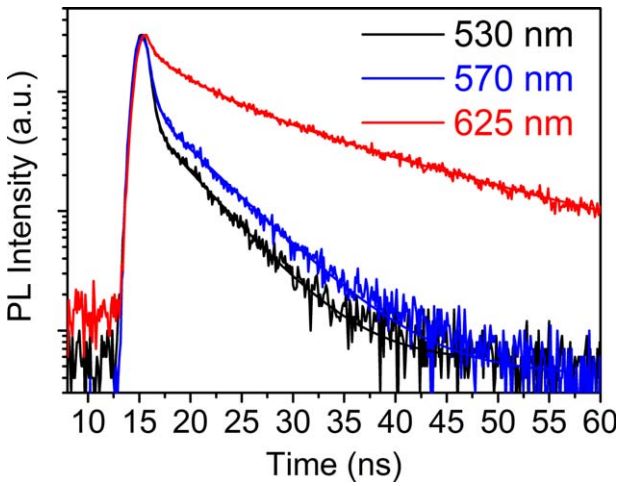

Figure 5. Time-resolved PL decays of the PDI in the polymer in THF obtained by pumping at 460 nm and probing at 530, 570, and 625 nm, respectively. [Color figure can be viewed in the online issue, which is available at wileyonlinelibrary.com.]

The PLE spectrum measured at the monitoring emission wavelength of 625 nm is markedly different from other two PLE spectra. Obviously, the origin of the excited states with the emission peak at 625 nm is different from those of the other excited states. The 625-nm PLE band is consistent with the experimental and theory absorption bands of the PDI coaxial dimmers, in which two PDI aromatic rings are parallelly stacked by π–π interaction.[30] The schematic structure of the π–π stacked dimmer is shown in the inset in Figure 4. The specific absorption band indicates that the 625 nm excited state is not excimers, but the π–π stacked aggregates of the PDI. Comparison with the absorption spectra in Figure 2, it can be found that the PDI is in favor of forming the π–π stacked aggregates in the polymer THF solution.

The properties of the excited states can be further analyzed by the time-resolved PL decays. Figure 5 shows the time-resolved PL decays of the PDI in the polymer in THF by probing at 530, 570, and 625 nm. Analysis of the time-resolved PL decays at 530 and 570 nm in terms of a sum of two exponential decays yields a good fit to the data, indicating the involvement of at least two deactivation processes for the 530 and 570 nm excited states. There is a short-lived process ($\tau_1 = 0.5 \pm 0.1$ ns with amplitude $a_1 = 0.24$) and a spontaneous radiative process ($\tau_2 = 5.0 \pm 0.5$ ns with $a_2 = 0.76$) for the 530 nm decay, correspondingly, the short-decay process (τ_1 with $a_1 = 0.20$) and the spontaneous radiative process (τ_2 with $a_2 = 0.80$) have been found in the 570 nm decay. Since, the fluorene moieties are adjacent to PDIs in the polymer backbone, the electron transfer between them can occur, which results in the nonradiative process (τ_1) in the PDIs. The life times of the 530 and 570 nm excited states are consistent with those of the PDI molecules in dilute solutions reported in Refs. 29,31 thus, it is reasonable to believe that the 530 and 570 nm emissions originate from the excited states with different energy levels in the separated PDIs in the polymer solution. Different from the PL decays at 530 and 570 nm, analysis of the time-resolved PL decays at 625 nm in terms of a sum of three exponential decays yields a good fit to the data, in which there is the short-lived process (τ_1 with $a_1 = 0.02$) and two spontaneous radiative processes (τ_2 with $a_2 = 0.23$ and $\tau_3 = 17.7$ ns with $a_3 = 0.75$). The long life time of the excited states is 17.7 ns, corresponding to the life time of the π–π stacked aggregates of the PDI.[28] Since, the π-electrons delocalize across the two coaxial PDIs, the molecular interactions broaden the energy band of the coaxial aggregates to reduce its energy gap. The life time of the excited states in the coaxial π–π stacked aggregates becomes long due to slow lattice relaxation caused by π-electron transition.

By comparison with the PL spectra of the PDI in the polymer solutions, it can be found that the luminescence efficiency of the PDI is decreases in THF because of forming the π–π stacked aggregates of the PDI with low luminescence efficiency in the coiled polymer chains. Obviously, the nonsolvent ethanol adding into the THF solution can make the polymer chains become coiled, and then collapsed due to the repulsive force of the nonsolvent. It can be seen from Figure 6 that the PL intensities of the PDI in the polymer in the blend solvents are decreased with the increase in the content of ethanol. The inset in Figure 6 shows the UV–vis absorption spectra of the PDI in the polymer in the blend solvents. The absorption intensity of the PDI is decreased with the increase in the content of ethanol. It is noteworthy, that the relative absorption intensity at 520 nm is markedly decreased. According to the PLE spectra in Figure 4, the 520 nm absorption band originates from the separated PDIs. The deceased absorption intensity at 520 nm implies that the separated PDIs are decreased with the added ethanol due to the formation of the PDI π–π stacked aggregates. It can be found that the shape of the absorption spectrum of the PDI in the polymer in THF/ethanol (v/v, 50%) blend solvent is similar to that of the 625 nm PLE spectrum. The results indicate that the π–π stacked aggregates of the PDI are increased in the collapsed

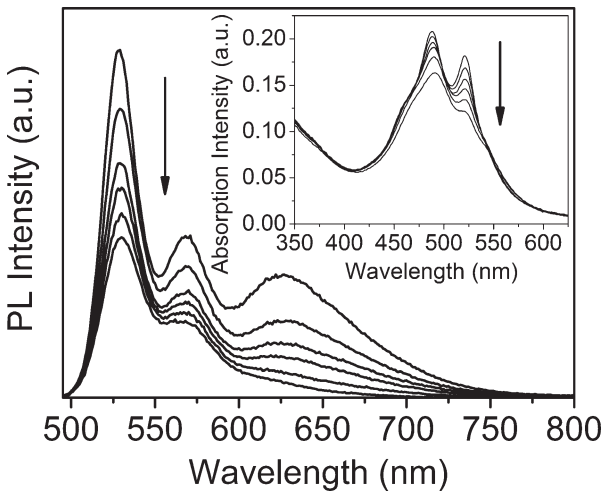

Figure 6. PL spectra of the PDI in the polymer in the blend solvents with the concentration of 5×10^{-4} mg/ml (excitation at 480 nm), the inset is the UV–vis absorption spectra of the PDI in the polymer in the blend solvents with the concentration of 5×10^{-3} mg/ml. The contents of ethanol (v/v) in the blend solvents are increased from 0% to 50% as the arrows show.

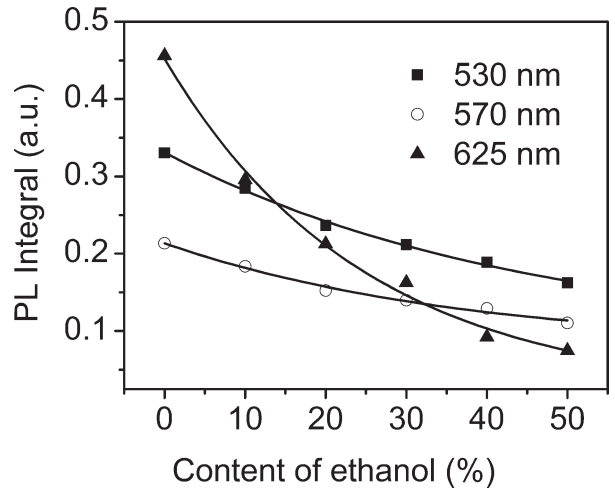

Figure 7. Solent dependent PL integrals of the three emission bands with the PL peaks at 530, 570, and 625 nm.

polymer chains in the THF/ethanol blend solvents. Although more π–π stacked aggregates are formed in the polymer THF/ethanol solutions, the PL intensity at 625 nm is markedly decreased with the increase in the content of ethanol. The concentration quenching can heavily decrease the PL intensity of the PDI π–π stacked aggregates.

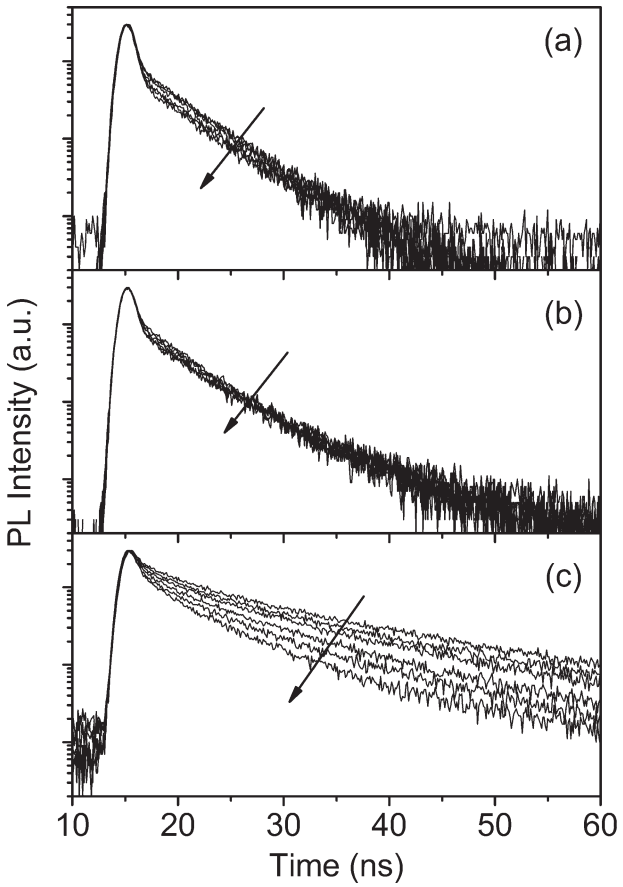

Figure 8. Time-resolved PL decays of the PDI in the polymer in THF/ethanol blend solvents obtained by pumping at 460 nm and probing at (a) 530 nm, (b) 570 nm, and (c) 625 nm, respectively. The contents of ethanol (v/v) in the blend solvents are increased from 0% to 50% as the arrows show.

Further analyzing the effect of the solvent on the PL spectra of the PDI in the polymer solutions, the relative PL integral intensities of the three emission bands with the PL peaks at 530, 570, and 625 nm are plotted in Figure 7 according to Gaussian fitting the PL spectra in Figure 6. Here, the PL integral intensity of the PDI in THF is considered as the reference. It can be seen that the contributions of the three excited states to the decreased PL integral intensity are different. The emission intensities of the 530 and 570 nm excited states are decreased with a similar trend, but the emission intensity of the 625 nm excited state is precipitately decreased with the increase of ethanol in the solution. The main reason for the decreased PL intensities at 530 and 570 nm is the collapsed polymer chains leading to decrease the separated PDIs. As above discussion, the polymer chains become collapsed as the content of the nonsolvent is increased in the blend solvent to result in forming more π–π stacked aggregates of the PDI. The precipitately decreased emission intensity at 625 nm indicates that the π–π stacked aggregates of the PDI are sensitive to the concentration of the chromophore.

Figure 8 shows the time-resolved PL decays of the 530, 570, and 625 nm excited states of the PDI in the polymer in the blend solvents. It can be found that the PL decays of the 530 and 570 nm excited states are not affected by adding ethanol. The results indicate that the added ethanol does not change the decay process of the excited states in the separated PDIs. The PL decays at 625 nm are obviously dependent on the content of ethanol in the blend solvents. According to the fitting data in term of a sum of three exponential decays, the amplitude of the short-lived component (τ_1) is increased with the increase in the content of ethanol, whereas the amplitude of the long-lived component (τ_3) is decreased. Thus, the added ethanol in the solution inducing the formation of the π–π stacked aggregates results in the increased concentration of the PDI aggregates and leads to increase the nonradiative recombination process. Thus, the concentration quenching leads to the quick PL decay, corresponding to the decreased PL intensity of the PDI π–π stacked aggregates in the blend solvents.

CONCLUSION

The optical properties of the PDI in the polymer are dependent on the solvent. The polymer chains become coiled in THF to result in the forming of the π–π stacked aggregates of the PDI, which contributes to the enhanced emission band with the PL peak at 625 nm. The PL intensity of the π–π stacked aggregates is precipitately decreased with the increase in the content of ethanol in the blend solvent. The time-resolved PL decays indicate that the decay processes of the 530 and 570 nm excited states are not affected by adding ethanol. The PL decays at 625 nm indicate that the nonradiative recombination process of the π–π stacked aggregates is increased the in the blend solvents. The PL intensity at 625 nm of the π–π stacked aggregates

induced by solvent in the collapsed polymer chains is precipitately decreased due to the concentration quenching.

ACKNOWLEDGEMENTS

This work was supported jointly by the National Natural Science Foundation of China under Grant No. 51071045, the Specialized Research Fund for the Doctoral Program of Higher Education under Grant No. 200802861065, and the Technology Fund of Southeast University under Grant No. KJ20100431.

REFERENCES

1. Struijk, C. W.; Sieval, A. B.; Dakhorst, J. E. J.; van Dijk, M.; Kimkes, P.; Koehorst, R. B. M.; Donker, H.; Schaafsma, T. J.; Picken, S. J.; van de Craats, A. M.; Warman, J. M.; Zuilhof, H.; Sudhöter, E. J. R. *J. Am. Chem. Soc.* **2000**, *122*, 11057.
2. Bendikov, M.; Wudl, F.; Perepichka, D. F. *Chem. Rev.* **2004**, *104*, 4891.
3. Wöll, D. H.; Uji-i, S. T.; Hotta, J.; Dedecker, P.; Herrmann, A.; De Schryver, F. C.; Müllen, K.; Hofkens, J. *Angew. Chem. Int. Ed.* **2008**, *47*, 783.
4. Chen, Z.; Baumeister, U.; Tschierske, C.; Würthner, F. *Chem. Eur. J.* **2007**, *13*, 450.
5. Wicklein, A.; Lang, A.; Muth, M.; Thelakkat, M. *J. Am. Chem. Soc.* **2009**, *131*, 14442.
6. Baggerman, J.; Jagesar, D. C.; Vallée, R. A. L.; Hofkens, J.; De Schryver, F. C.; Schelhase, F.; Vögtle, F.; Brouver, A. M. *Chem. Eur. J.* **2007**, *13*, 1291.
7. Gebers, J.; Rolland, D.; Frauenrath, H. *Angew. Chem. Int. Ed.* **2009**, *48*, 4480.
8. Mareda, J.; Matile, S. *Chem. Eur. J.* **2009**, *15*, 28.
9. Schmidt-Mende, L.; Fechtenkötter, A.; Müllen, K.; Moons, E.; Friend, R. H.; MacKenzie, J. D. *Science* **2001**, *293*, 1119.
10. Herrmann, A.; Müllen, K. *Chem. Lett.* **2006**, *35*, 978.
11. Grimsdale, A. C.; Müllen, K. *Angew. Chem. Int. Ed.* **2005**, *44*, 5592.
12. Ego, C.; Marsitzky, D.; Becker, S.; Zhang, J. Y.; Grimsdale, A. C.; Müllen, K.; MacKenzie, J. D.; Silva, C.; Friend, R. H. *J. Am. Chem. Soc.* **2003**, *125*, 437.
13. Lang, A. S.; Neubig, A.; Sommer, M.; Thelakkat, M. *Macromolecules* **2010**, *43* 7001.
14. Zhan, X. W.; Tan, Z. A.; Domercq, B.; An, Z. S.; Zhang, X.; Barlow, S.; Li, Y. F.; Zhu, D. B.; Kippelen, B.; Marder, S. R. *J. Am. Chem. Soc.* **2007**, *129*, 7246.
15. Bu, L. J.; Guo, X. Y.; Yu, B.; Qu, Y.; Xie, Z. Y.; Yan, D. H.; Geng, Y. H.; Wang, F. S. *J. Am. Chem. Soc.* **2009**, *131*, 13242.
16. Schenning, A. P. H. J.; Herrikhuyzen, J. V.; Jonkheijm, P.; Chen, Z. J.; Würthner, F.; Meijer, E. W. *J. Am. Chem. Soc.* **2002**, *124*, 10252.
17. Jonkheijm, P.; Stutzmann, N.; Chen, Z. J.; de Leeuw, D. M.; Meijer, E. W.; Schenning, A. P. H. J.; Würthner, F. *J. Am. Chem. Soc.* **2006**, *128*, 9535.
18. Fron, E.; Deres, A.; Rocha, S.; Zhou, G.; Müllen, K.; De Schryver, F. C.; Sliwa, M.; Uji-i, H.; Hofkens, J.; Vosch, T. *J. Phys. Chem. B* **2010**, *114*, 1277.
19. Williams, M. E.; Murray, W. R. *Chem. Mater.* **1998**, *10*, 3603.
20. Neuteboom, E. E.; Meskers, S. C. J.; Meijer, E. W.; Janssen, R. A. *J. Macromol. Chem. Phys.* **2004**, *205*, 217.
21. Bodapati, J. B.; lcil, H. *Dyes Pigments* **2008**, *79*, 224.
22. Cazacu, M.; Vlada, A.; Airineia, A.; Nicolescua A.; Stoica, I. *Dyes Pigments* **2011**, *90*, 106.
23. Niu, H.; Wang, C.; Bai, X. D.; Huang, Y. *J. Mater. Sci.* **2004**, *39*, 4053.
24. Tokumitsu, K.; Tanaka, A.; Kobori, K.; Kozono, Y.; Yamada, M.; Nitta, K. H. *J. Polym. Sci. B: Polym. Phys.* **2005**, *43*, 2259.
25. Yuan, Y.; Lin, B. P.; Zhang, X. Q.; Wu, L. W.; Zhan, Y. *J. Appl. Polym. Sci.* **2008**, *110*, 1515.
26. Yang, C. P.; Lin, J. H. *J. Polym. Sci.: Polym. Chem.* **1993**, *31*, 2153.
27. Valeur, B. Molecular Fluorescence: Principles and Applications. Wiley-VCH Verlag GmbH: Weinheim, **2001**.
28. Veldman, D.; Chopin, S. M. A.; Meskers, S. C. J.; Groeneveld, M. M.; Williams, R. M.; Janssen, R. A. J. *J. Phys. Chem. A* **2008**,*112*, 5846.
29. Spreitler, F.; Sommer, M.; Thelakkat, M.; Köhler, J. *Phys. Chem. Chem. Phys.* **2012**, *14*, 7971.
30. Giaimo, J. M.; Lockard, J. V.; Sinks, L. E.; Scott, A. M.; Wilson, T. M.; Wasielewski, M. R. *J. Phys. Chem. A* **2008**, *112*, 2322.
31. Xiao, S. Q.; El-Khouly, M. E.; Li, Y. L.; Gan, Z. H.; Liu, H. B.; Jiang, L.; Araki, Y.; Ito, O.; Zhu, D. B. *J. Phys. Chem. B* **2005**, *109*, 3658.